

# Integrin Acts Upstream of Netrin Signaling to Regulate Formation of the Anchor Cell's Invasive Membrane in *C. elegans*

Elliott J. Hagedorn,<sup>1</sup> Hanako Yashiro,<sup>2</sup> Joshua W. Ziel,<sup>1</sup> Shinji Ihara,<sup>1</sup> Zheng Wang,<sup>1</sup> and David R. Sherwood<sup>1,3,\*</sup>

<sup>1</sup>Department of Biology, Duke University, Science Drive, Box 90388, Durham, NC 27708, USA

<sup>2</sup>Washington University School of Medicine, Center for Pharmacogenetics, Box 8086, 660 South Euclid Avenue, St. Louis, MO 63110, USA

<sup>3</sup>Molecular Cancer Biology Program, Duke University Medical Center, Durham, NC 27708, USA

\*Correspondence: david.sherwood@duke.edu

DOI 10.1016/j.devcel.2009.06.006

## SUMMARY

Integrin expression and activity have been strongly correlated with developmental and pathological processes involving cell invasion through basement membranes. The role of integrins in mediating these invasions, however, remains unclear. Utilizing the genetically and visually accessible model of anchor cell (AC) invasion in *C. elegans*, we have recently shown that netrin signaling orients a specialized invasive cell membrane domain toward the basement membrane. Here, we demonstrate that the integrin heterodimer INA-1/PAT-3 plays a crucial role in AC invasion, in part by targeting the netrin receptor UNC-40 (DCC) to the AC's plasma membrane. Analyses of the invasive membrane components phosphatidylinositol 4,5-bisphosphate, the Rac GTPase MIG-2, and F-actin further indicate that INA-1/PAT-3 plays a broad role in promoting the plasma membrane association of these molecules. Taken together, these studies reveal a role for integrin in regulating the plasma membrane targeting and netrin-dependent orientation of a specialized invasive membrane domain.

## INTRODUCTION

Basement membranes (BMs) are thin, dense, and highly cross-linked forms of extracellular matrix that provide the structural underpinning for all epithelia, endothelia, and many mesenchymal cells in metazoans (Kalluri, 2003; Rowe and Weiss, 2008; Yurchenco et al., 2004). Despite its barrier properties, numerous cells during development and in normal physiological processes undergo highly regulated invasions through BMs to disperse, form tissues, and mediate immune system responses (Hughes and Blau, 1990; Risau, 1997; Wang et al., 2006). Metastatic cancer cells are thought to exploit the same underlying regulatory networks to breach BMs during their spread to distant tissues (Friedl and Wolf, 2003). Efforts to elucidate the genetic pathways that control invasive behavior have been limited by the experimental inaccessibility of cell-matrix interactions in the complex and dynamic in vivo tissue environments where

cell invasions occur (Even-Ram and Yamada, 2005; Hotary et al., 2006; Wang et al., 2006). As a result, the mechanisms that promote cell invasion through BMs during development and cancer remain poorly understood (Machesky, 2008; Rowe and Weiss, 2008).

Anchor cell (AC) invasion into the vulval epithelium in *C. elegans* is an in vivo model of invasive behavior that allows for genetic and single-cell visual analysis of invasion (Sherwood et al., 2005; Sherwood and Sternberg, 2003). During the mid-L3 larval stage, a basally derived invasive process from the AC crosses the gonadal and ventral epidermal BMs and then moves between the central 1°-fated vulval precursor cells (VPCs) to mediate uterine-vulval attachment (Sharma-Kishore et al., 1999; Sherwood and Sternberg, 2003). Recent studies have shown that the invasive cell membrane of the AC is a specialized subcellular domain that is polarized toward the BM by the action of the UNC-6 (netrin) pathway (Ziel et al., 2009). Approximately 4 hr prior to invasion, expression of the secreted guidance cue UNC-6 (netrin) from the ventral nerve cord targets its receptor, UNC-40 (DCC), to the AC's invasive membrane. There, netrin signaling localizes a number of actin regulators that promote invasion, including the Rac GTPases MIG-2 and CED-10, the Ena/VASP ortholog UNC-34, and the phospholipid phosphatidylinositol 4,5-bisphosphate (PI(4,5)P<sub>2</sub>) (Ziel et al., 2009). The proper orientation of these components at the basal membrane is required to generate robust protrusions that breach the BM in response to a later cue from the 1° VPCs that stimulates invasion. Although the molecular components of the invasive membrane are misoriented in *unc-6* mutants, they still associate in a nonpolarized manner with the AC's plasma membrane, suggesting that a distinct mechanism exists for regulating their targeting to the cell membrane.

Integrins are one of the major cell surface receptors used by metazoan cells to mediate direct cell-matrix interactions (Yurchenco et al., 2004). All integrins are heterodimers composed of a single  $\alpha$  and  $\beta$  subunit. In vertebrates, integrins have been implicated in regulating cell invasion during blastocyst implantation, angiogenesis, and leukocyte trafficking (Hodivala-Dilke, 2008; Sixt et al., 2006; Staun-Ram and Shalev, 2005). Furthermore, the dysregulation of integrin expression and function has been associated with a number of metastatic cancers (Felding-Habermann, 2003; Hood and Cheresh, 2002). Mammals utilize 18  $\alpha$  and 8  $\beta$  subunits, which combine to form an array of different heterodimers (Hood and Cheresh, 2002). The complexity of the

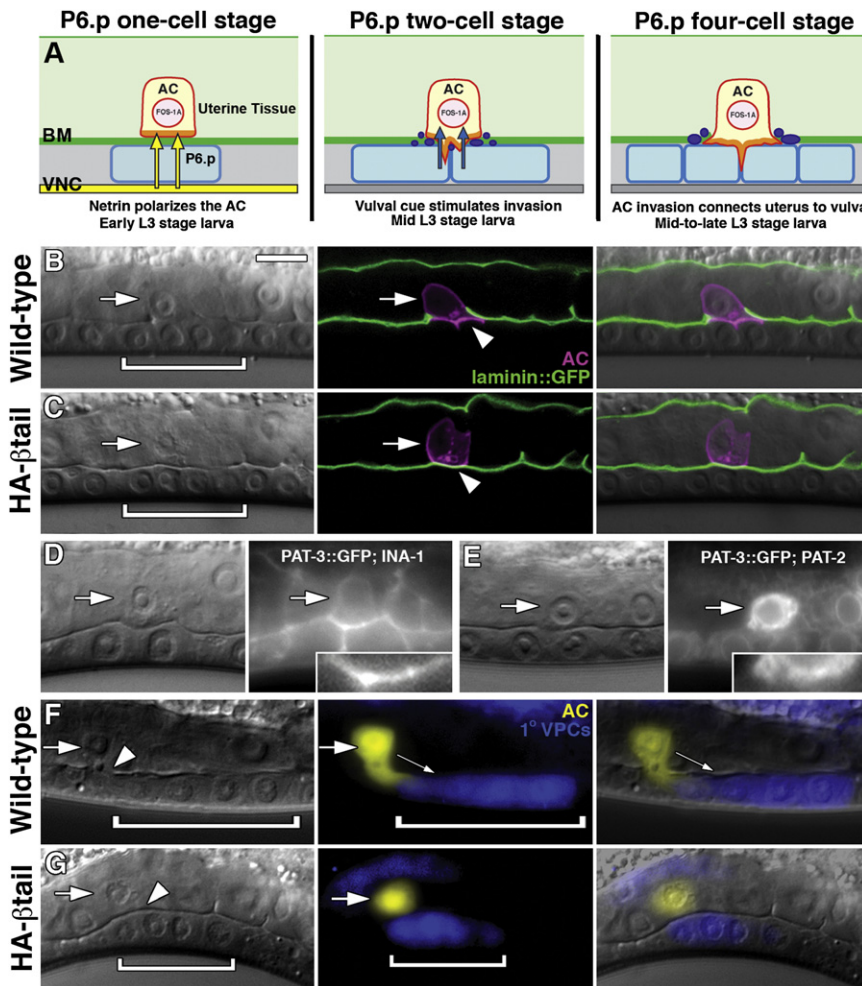


**Figure 1. The INA-1/PAT-3 Integrin Heterodimer Mediates AC Invasion**

Anterior is oriented toward the left, and ventral is down; brackets designate 1° VPCs, and arrows point to AC in this and all other figures.

(A) Schematic diagram depicting wild-type AC invasion. In the early-L3 larval stage (left), UNC-6 (netrin, yellow arrows) secreted from the ventral nerve cord (VNC) polarizes the AC's invasive membrane domain (orange) toward the basement membrane (BM). During the mid-L3 larval stage (middle), the 1° VPC-fated P6.p cell daughters generate a chemotactic cue (blue arrows, center) that stimulates the extension of invasive protrusions from the AC that breach the BM and contact the P6.p granddaughters (right). Targets of the transcription factor FOS-1A, including hemicentin (purple puncta), regulate the removal of BM during invasion.

(B) Nomarski (left), fluorescence (center), and overlaid images (right) of a wild-type animal show the AC (expressing *cdh-3* > mCherry::PLCδ<sup>PH</sup>, magenta) invading through the BM (arrowhead, visualized by the laminin marker LAM-1::GFP, green).

(C) HA-βtail expression blocked invasion, and the AC remained associated with an intact BM (arrowhead; see Movies S1 and S2).

(D) The β integrin subunit PAT-3::GFP was localized to the AC's surface and concentrated at the invasive cell membrane (inset magnification) when cotransformed with the α integrin subunit *ina-1*.

(E) PAT-3::GFP was internally localized after cotransformation with the α integrin subunit *pat-2* (inset magnification).

(F) A wild-type AC (expressing *cdh-3* > YFP, yellow) extending an invasive process (small arrow) through the BM (arrowhead) toward displaced 1° VPCs (expressing *egl-17* > CFP, blue).

(G) ACs expressing HA-βtail failed to extend invasive processes toward displaced 1° VPCs, even when bordered by 1° VPCs.

The scale bar represents 5 μm in this and all other figures.

mammalian integrin receptor family, combined with the difficulty of in vivo analysis has hindered an understanding of the requirement and function of integrin receptors in mediating BM invasion (Felding-Habermann, 2003; Friedl and Wolf, 2003; Sixt et al., 2006). *C. elegans* possess only two predicted integrin receptors, composed of an α PAT-2 or α INA-1 subunit bound with the sole β subunit, PAT-3 (Kramer, 2005), providing a simplified genetic landscape for examining integrin function.

We have conducted an RNAi screen to identify additional pathways that regulate invasion, and we report here that the *C. elegans* integrin heterodimer INA-1/PAT-3 is a crucial regulator of AC invasion. Cell biological and genetic analyses indicate that INA-1/PAT-3 functions within the AC to control the formation of invasive protrusions that breach the BM. Our analysis identifies a key role for integrin in regulating the membrane association of components of the invasive cell membrane, including the netrin receptor UNC-40 (DCC). This work demonstrates an essential role for integrin in controlling BM invasion and reveals an integrin-netrin pathway interaction that mediates the mem-

brane targeting and polarization of the molecular constituents of the AC's invasive membrane.

## RESULTS

### Summary of AC Invasion into the Vulval Epithelium

During the early-L3 larval stage, the gonadal AC is separated from the underlying P6.p VPC by the juxtaposed gonadal and ventral epidermal BMs. At this time, UNC-6 (netrin) secreted by the ventral nerve cord orients a specialized F-actin-rich, invasive cell membrane domain within the AC toward the BM (P6.p one-cell stage; Figure 1A). Approximately 4 hr later, the underlying 1°-fated P6.p cell divides (P6.p two-cell stage) and produces an unidentified cue, which stimulates the formation of invasive protrusions that breach the BM and contact the P6.p granddaughters (P6.p four-cell stage; Figures 1A and 1B). Breaching the BM is dependent upon the transcription factor FOS-1A, which regulates the expression of genes in the AC that mediate BM removal (Hwang et al., 2007; Rimann and Hajnal, 2007;

**Table 1. Genetic Analysis of Integrin Function in AC Invasion**

Genotype/Treatment	ACs Showing Full, Partial, or No Invasion <sup>a</sup>							
	P6.p Four-Cell Stage (Mid-to-Late L3 Stage)				P6.p Eight-Cell Stage (Early-L4 Stage)			
	% Full Invasion	% Partial Invasion	% No Invasion	n	% Full Invasion	% Partial Invasion	% No Invasion	n
Wild-type (N2)	100	0	0	100	100	0	0	100
<b>Integrin</b>								
<i>ina-1(RNAi); rrf-3(pk1426)</i> <sup>b</sup>	66	12	22	74	99	1	0	75
<i>pat-3(RNAi); rrf-3(pk1426)</i> <sup>b,c</sup>	16	26	58	82	28	35	37	54
<i>talin(RNAi); rrf-3(pk1426)</i> <sup>b</sup>	38	37	25	60	86	12	2	58
<i>pat-4(RNAi); rrf-3(pk1426)</i> <sup>b</sup>	75	20	5	55	100	0	0	57
<i>pat-2(RNAi); rrf-3(pk1426)</i> <sup>b</sup>	100	0	0	31	100	0	0	45
<i>ina-1(gm39)</i>	32	18	50	116	74	3	22	135
<i>ina-1(gm144)</i>	100	0	0	103	100	0	0	113
<i>qyEx4[zmp-1 &gt; HA-βtail]</i> <sup>d</sup>	21	6	73	102	49	3	48	101
<i>qyEx35[zmp-1 &gt; HA-βΔ]</i> <sup>d</sup>	100	0	0	52	100	0	0	50
<i>qyls15[zmp-1 &gt; HA-βtail]</i>	0	4	96	100	9	10	81	123
<i>qyls48[zmp-1 &gt; HA-βtail]</i>	0	3	97	62	24	26	50	101
<i>qyls110[egl-17 &gt; HA-βtail]</i>	100	0	0	90	100	0	0	65
<i>pat-3 (RNAi); qyls103[fos-1a &gt; rde-1]; rde-1; rrf-3(pk1426)</i> <sup>b</sup>	44	34	22	56	77	23	0	53
<b>Netrin Pathway Interactions</b>								
<i>unc-40(e271)</i>	5	20	75	57	72	8	20	50
<i>unc-40(e271); ina-1(gm39)</i>	0	0	100	100	5	12	83	53
<b>fos-1 Pathway Interactions</b>								
<i>fos-1(ar105)</i>	0	0	100	30	1	26	73	66
<i>fos-1(ar105); ina-1(RNAi)</i>	0	0	100	25	0	8	92	63
<i>zmp-1(cg115)</i>	100	0	0	50	100	0	0	50
<i>zmp-1(cg115); qyls48[pACz &gt; HA-βtail]</i>	0	3	97	100	21	23	56	111
<i>him-4(rh319)</i>	80	7	13	100	96	1	3	100
<i>qyls15[pACz &gt; HA-βtail]; him-4(rh319)</i>	0	2	98	100	7	9	84	104

<sup>a</sup> Full, partial, and no AC invasion was determined by examination of the phase dense line separating the uterine and vulval tissue under Nomarski optics. This phase dense line is formed by an intact basement membrane, and during wild-type AC invasion it is interrupted (see Figure S1).

<sup>b</sup> The *rrf-3* mutant background is more sensitive to somatic RNAi effects. All ACs that failed to invade after this treatment remained attached to the BM.

<sup>c</sup> To bypass the embryonic lethality of *pat-3* RNAi, L1-arrested larva were grown for 5 hr on regular OP50 bacteria in the absence of RNAi. The worms were then transferred to bacteria expressing *pat-3* dsRNAi.

<sup>d</sup> Two additional transgenic lines with these same transgenes showed similar results.

Sherwood et al., 2005). AC invasion is completed at the L3 molt when the basolateral portion of the AC moves between the P6.p great-granddaughters at the apex of the vulva (P6.p eight-cell stage; see Figure S1 available online). AC invasion initiates uterine-vulval attachment, and its timing and targeting are invariant in wild-type animals (Sherwood and Sternberg, 2003).

### INA-1/PAT-3 Integrin Signaling Regulates AC Invasion

Ablation of the AC just prior to invasion disrupts uterine-vulval attachment and results in a protruded vulval (Pvl) phenotype (Kimble, 1981; Seydoux et al., 1993). To identify genes that regulate invasion, we examined genes whose knockdown by bacterial feeding of RNAi has been reported to produce a Pvl phenotype (Kamath et al., 2003) and found that RNAi targeting the  $\alpha$  integrin subunit *ina-1* resulted in an AC invasion defect (Table 1). Null mutations in *ina-1* cause L1 larval lethality (Baum and Garriga, 1997). We therefore examined two hypomorphic

mutations in *ina-1*, *ina-1(gm39)* and *ina-1(gm144)*, that appear to affect different functions of *ina-1* (Baum and Garriga, 1997). *ina-1(gm39)* mutants, which harbor a missense mutation within the putative ligand-binding  $\beta$  propeller region of the protein, had a significant invasion defect, with 50% of ACs showing a lack of invasion at the P6.p four-cell stage, and 22% failing to invade by the P6.p eight-cell stage (Figure S1; Table 1). In contrast, *ina-1(gm144)* animals, which contain a distinct missense lesion adjacent to the transmembrane domain (a region that might regulate integrin affinity for its ligand) had normal AC invasion despite this allele causing neuronal migration defects (Baum and Garriga, 1997) (Table 1). These results confirm a role for *ina-1* in regulating AC invasion, and they provide further evidence of separable *ina-1* functions.

In both *Drosophila* and vertebrates,  $\alpha$  and  $\beta$  integrin subunits require heterodimerization within the secretory apparatus to be transported to the cell surface (Leptin et al., 1989; Marlin et al.,



1986). Consistent with a similar regulatory mechanism in *C. elegans*, high levels of full-length transgenes encoding the sole  $\beta$  integrin, PAT-3::GFP, or the  $\alpha$  integrin INA-1::GFP alone showed internal localization within the AC, as well as in neighboring somatic gonad and vulval cells (Figure S2). Cotransformation of *pat-3::GFP* with genomic DNA encoding INA-1 resulted in PAT-3::GFP localization to the cell surface with increased levels at the AC's invasive cell membrane (Figure 1D), indicating that INA-1 forms a heterodimer with PAT-3 in the AC. Cotransformation with genomic DNA encoding the other *C. elegans*  $\alpha$  subunit, PAT-2, did not result in translocation of PAT-3::GFP to the cell surface (Figure 1E). Further analysis with a translational PAT-2::GFP fusion revealed that *pat-2* was not expressed in the AC at the time of invasion (Figure S2), and RNAi-mediated depletion of *pat-2* did not perturb AC invasion (Table 1). These results strongly suggest that the  $\alpha$  subunit PAT-2 does not regulate AC invasion.

To further investigate a role for integrin signaling during AC invasion, we used RNAi to target two major downstream effectors of integrin signaling, *talin* and *pat-4* (ILK). RNAi depletion of each of these genes resulted in a defect in AC invasion (Table 1). Notably, RNAi targeting *talin* resulted in a stronger invasion defect than RNAi to *pat-4* (ILK), consistent with the former being a more essential component of the integrin signaling pathway (Delon and Brown, 2007). Taken together, these results indicate that the integrin  $\alpha$  subunit *ina-1* and core components of the integrin pathway promote AC invasion.

### PAT-3 Functions within the AC to Promote Invasion

To determine where integrin signaling functions during AC invasion, we first used a tissue-specific RNAi strain, *fos-1a > rde-1*, in which only the uterine tissue (which includes the AC) is sensitive to RNAi (see Supplemental Experimental Procedures). Treatment of *fos-1a > rde-1* animals with RNAi targeting the sole  $\beta$  integrin, *pat-3*, resulted in a defect in AC invasion (Table 1). These results indicate that PAT-3 functions within the uterine tissue during AC invasion, consistent with a direct role in the AC.

To determine if *pat-3* functions within the AC, we disrupted *pat-3* function here by utilizing a previously characterized dominant-negative construct encoding the PAT-3 transmembrane and cytoplasmic domains connected to a heterologous hemagglutinin (HA) extracellular domain (HA- $\beta$ tail) (Lee et al., 2001). Autonomous expression of the  $\beta$  integrin cytoplasmic domain has been shown to act as a dominant-negative inhibitor of endogenous integrin function (LaFlamme et al., 1994; Lukashev et al., 1994; Martin-Bermudo and Brown, 1999). We expressed the HA- $\beta$ tail construct by using the AC-specific *zmp-1* promoter, which initiates expression before invasion at the late-L2 stage and drives increasing levels in the AC up to the time of invasion (Figure S3). At the P6.p four-cell stage, when AC invasion normally occurs, >70% of transgenic HA- $\beta$ tail animals failed to invade, and ~50% of ACs failed to invade by the P6.p eight-cell stage (Figure S3; Table 1). The stable chromosomal integration of *zmp-1 > HA- $\beta$ tail (qyls15 and qyls48)* led to nearly a complete block in invasion at the P6.p four-cell stage (Table 1). Confirming the specificity of this perturbation, AC invasion was normal in animals expressing a control construct (*zmp-1 > HA- $\beta$ 4*), which lacks the cytoplasmic signaling domain of  $\beta$  integrin (Table 1; see Supplemental Experimental Procedures). Further-

more, expression of HA- $\beta$ tail under the control of the 1° VPC-specific promoter *egl-17* did not affect AC invasion (Table 1). Finally, mosaic analysis with PAT-3::GFP expression to rescue the *pat-3* null mutant *pat-3(rh54)* further indicated that *pat-3* functions within the AC, but not the vulval cells, to regulate invasion (Figure S4). Taken together, these results indicate that PAT-3 function is required within the AC to promote invasion.

### The AC Associates with the BM after Perturbation of INA-1/PAT-3 Signaling

*ina-1* encodes an integrin most similar to vertebrate and *Drosophila* integrins that bind the BM component laminin (Baum and Garriga, 1997). To determine if INA-1/PAT-3 might mediate AC invasion by maintaining matrix attachment, we examined the interaction of the AC with the BM after perturbation of integrin signaling. We visualized the AC plasma membrane with the pleckstrin-homology (PH) domain from *phospholipase C- $\delta$*  fused to mCherry and driven by the AC-specific promoter *cdh-3* (*cdh-3 > mCherry::PLC $\delta^{PH}$* ) (Rescher et al., 2004). The BM was simultaneously observed with a functional laminin  $\beta$  subunit (LAM-1::GFP) (Kao et al., 2006). Similar to wild-type animals, ACs expressing HA- $\beta$ tail were in direct contact with the BM at the P6.p one- and two-cell stages leading up to invasion, and they remained attached to an intact BM after the time of normal invasion ( $\geq 20$  animals at each stage; Figures 1B and 1C; Movies S1 and S2). Notably, however, at the normal time of invasion there was a significant 27% reduction in the width of AC contact with the BM in HA- $\beta$ tail animals (from 7.2  $\mu$ m to 5.3  $\mu$ m;  $p < 0.05$ ; Student's *t* test), consistent with a role in modulating BM adhesion. In *ina-1(gm39)* mutants, ~10% of ACs were detached from the BM from the time of AC specification at the late-L2 stage up to the time of invasion (10/74 animals at the P6.p one-cell stage, and 6/81 animals at the P6.p two-cell stage), reflecting a possible earlier requirement in mediating BM association. The majority of ACs that failed to invade at the P6.p four-cell stage in *ina-1* mutants, however, were attached to an intact BM (66/74 animals). The AC also remained attached to the BM in all ACs that failed to invade after RNAi-mediated depletion of *ina-1*, *pat-3*, *pat-4* (ILK), and *talin* (Table 1). Taken together, these results suggest that INA-1/PAT-3 has an active role in promoting AC invasion that extends beyond mediating BM attachment.

### INA-1/PAT-3 Regulates the Protrusive Activity of the AC

AC invasion requires the generation of invasive processes that penetrate the BM in response to a chemotactic cue from the 1° VPCs (Sherwood and Sternberg, 2003). To examine whether INA-1/PAT-3 regulates this protrusive activity, we ablated all VPCs except the posterior most P8.p cell in wild-type and HA- $\beta$ tail animals containing *egl-17 > CFP* to visualize 1° VPC fate specification and the AC marker *cdh-3 > YFP*. Under these conditions, the descendants of P8.p adopt the 1° VPC fate and generate the chemotactic cue that stimulates invasion, thus providing an assay for the ability of the AC to generate processes toward displaced 1° VPCs (Sherwood and Sternberg, 2003). In wild-type animals, 80% of ACs initiated the extension of processes toward the isolated 1°-fated P8.p cell descendants at the P8.p two-cell stage (16/20 animals), and at the P8.p four-cell stage all ACs responded with an invasive process that breached BM (14/14 animals; Figure 1F). In contrast, only 35%

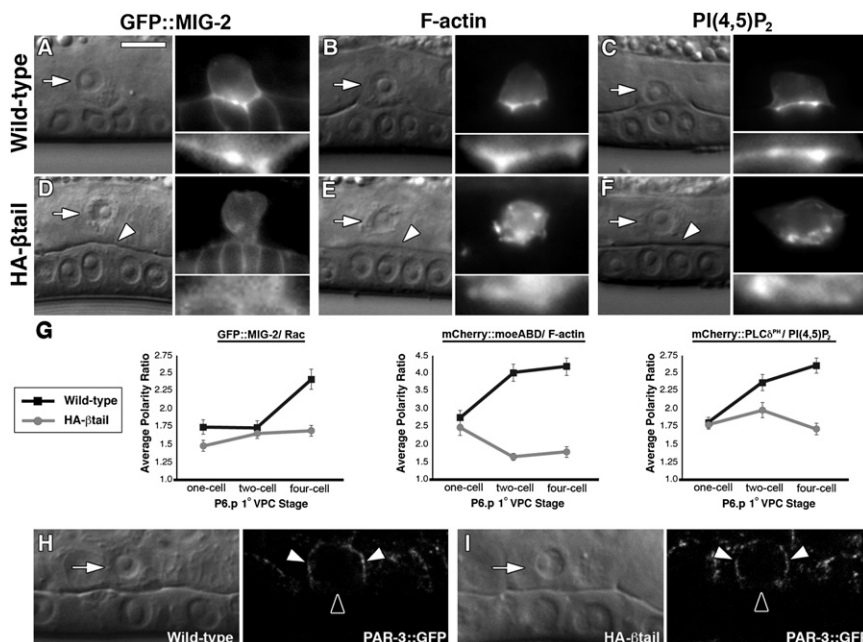


**Figure 2. INA-1/PAT-3 Promotes the Formation of the Invasive Cell Membrane**

Nomarski image (left); corresponding fluorescence (right).

(A–C) The Rac protein GFP::MIG-2, the F-actin binding probe mCherry::moeABD, and the phosphatidylinositol 4,5-bisphosphate (PI(4,5)P<sub>2</sub>) sensor mCherry::PLCδ<sup>PH</sup> localize to the invasive cell membrane of the AC in wild-type animals (insets show magnification of the invasive membrane in [A]–[F]). (D–F) AC-specific expression of HA-βtail blocked invasion (white arrowheads) and perturbed MIG-2, F-actin, and PI(4,5)P<sub>2</sub> localization to the invasive cell membrane.

(G) Quantification of MIG-2, F-actin, and PI(4,5)P<sub>2</sub> polarization in wild-type (black squares) and HA-βtail ACs (gray circles) at the P6.p one-, two-, and four-cell stages. In wild-type animals, MIG-2, F-actin, and PI(4,5)P<sub>2</sub> localization to the invasive membrane increased over time; however, in HA-βtail animals, their polarization did not change (MIG-2 and PI(4,5)P<sub>2</sub>) or decreased (F-actin;  $n \geq 15$  animals for each stage). Polarity of these invasive membrane components was significantly less at the P6.p four-cell stage in HA-βtail animals compared to wild-type ( $p < 2 \times 10^{-4}$ , Student's *t* test). Error bars report the standard error of the mean.

(H) The polarity marker PAR-3::GFP localized to apical and lateral membranes of wild-type ACs (white arrowheads), but not the invasive membrane (black arrowhead).

(I) PAR-3::GFP localization was normal in HA-βtail animals.

of ACs in HA-βtail animals initiated the extension of processes at the P8.p two-cell stage (6/17 animals), and less than 20% did so at the P8.p four-cell stage (3/16 animals), with most ACs failing to generate protrusions (Figure 1G). Furthermore, of the few processes observed, none breached the BM (3/3 animals). These results suggest that INA-1/PAT-3 mediates AC invasion, at least in part by regulating the protrusive activity of the AC.

### INA-1/PAT-3 Promotes the Formation of the AC's Invasive Membrane

The proper formation of the AC's invasive cell membrane is required for the extension of invasive processes (Ziel et al., 2009). To determine whether INA-1/PAT-3 regulates invasive cell membrane formation, we examined the localization of a full-length GFP-tagged transgene of the *C. elegans* Rac ortholog MIG-2, as well as AC-specific expression of the F-actin marker mCherry::moeABD and the PI(4,5)P<sub>2</sub> reporter mCherry::PLCδ<sup>PH</sup>. In wild-type animals MIG-2, F-actin, and PI(4,5)P<sub>2</sub> are enriched at the invasive cell membrane at the P6.p one-cell stage, and their polarized localization increases through the time of invasion (Figures 2A–2C and 2G). In HA-βtail animals, MIG-2, F-actin, and PI(4,5)P<sub>2</sub> were polarized normally at the P6.p one-cell stage (Figure 2G). Notably, this was at the time when levels of the dominant-negative HA-βtail were low in the AC. After this initial establishment of polarity, however, as levels of HA-βtail increased, MIG-2 and PI(4,5)P<sub>2</sub> failed to further concentrate and there was a loss of F-actin polarity (Figures 2D–2G). The polarity of these molecules was similarly decreased after RNAi knockdown of *ina-1*, *pat-3*, or *taln*, but it was unaffected by the expression of

the dominant-negative control HA-βΔ, thus confirming the specificity of the dominant-negative HA-βtail (Figure S5; data not shown). These results suggest that INA-1/PAT-3 is required for the maturation of the invasive membrane, and that failure to generate protrusions in HA-βtail animals was a result of perturbation in this specialized membrane domain. Importantly, PAR-3::GFP, which localizes to apical and lateral membranes of wild-type ACs, and AJM-1::GFP, which is found in apical spot junctions, both localized normally in HA-βtail animals (Figures 2H and 2I; data not shown). Thus, INA-1/PAT-3 specifically regulates the invasive cell membrane, but not the overall polarity of the AC.

### UNC-40 Localization to the Invasive Membrane Is Dependent on INA-1/PAT-3

UNC-6 (netrin) secretion from the ventral nerve cord directs its receptor, UNC-40 (DCC), to the AC's basal cell membrane where netrin signaling functions to orient additional components of the invasive membrane (Ziel et al., 2009). To determine whether INA-1/PAT-3 might regulate invasive membrane formation through the netrin pathway, we examined the localization of UNC-40::GFP in wild-type and HA-βtail animals. Similar to F-actin and actin regulators (Figure 2G), UNC-40::GFP initially localized normally to the invasive cell membrane in HA-βtail animals (Figures 3A and 3B). This nascent polarity, however, was subsequently lost by the P6.p four-cell stage (Figures 3C–3G), and there was an apparent overall decrease in UNC-40::GFP membrane localization compared with wild-type ACs (Figure S6). The polarity of UNC-40::GFP was similarly perturbed

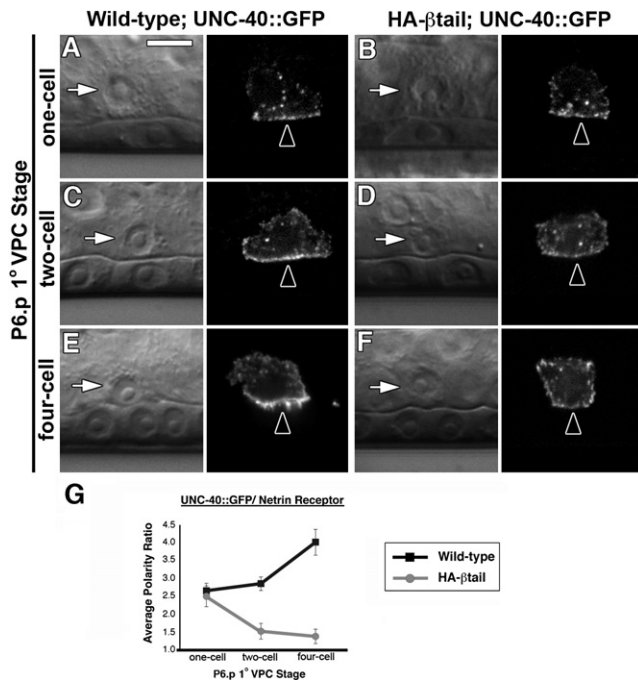


**Figure 3. INA-1/PAT-3 Regulates UNC-40 (DCC) Localization to the Invasive Cell Membrane**

Nomarski image (left); corresponding fluorescence (right).

(A, C, and E) UNC-40::GFP localized to the invasive membrane of the AC at the P6.p one-cell stage and increased its concentration there over time (black arrowheads).

(B, D, and F) In *HA- $\beta$ tail* animals, initial UNC-40::GFP-polarized localization at the P6.p one-cell stage was lost over time (black arrowheads).

(G) Quantification of UNC-40::GFP polarity in wild-type (black squares) and *HA- $\beta$ tail* ACs (gray circles) at the P6.p one-, two-, and four-cell stages ( $n \geq 15$  animals for each stage). UNC-40::GFP polarity in *HA- $\beta$ tail* ACs at the P6.p four-cell stage was significantly less than wild-type ( $p < 5 \times 10^{-3}$ , Student's *t* test). Error bars report the standard error of the mean.

after RNAi-mediated depletion of *ina-1*, *pat-3*, or *talin*, whereas polarity was normal in control *HA- $\beta$  $\Delta$*  animals (Figure S5). Conversely, INA-1/PAT-3::GFP was localized normally in both *unc-6(ev400)* and *unc-40(e271)* mutant animals (20/20 animals for each; Figure S7). These results suggest that INA-1/PAT-3 acts upstream of the netrin pathway in the AC to regulate invasive membrane formation.

#### Formation of the Invasive Membrane in *ina-1* Hypomorphs Correlates with Invasion

The hypomorphic mutant *ina-1(gm39)*, which has a weaker AC invasion phenotype than *HA- $\beta$ tail* animals (Table 1), allowed us next to determine the relationship between invasive membrane formation, UNC-40 localization, and the ability of the AC to invade. Strikingly, *ina-1(gm39)* mutant ACs that had UNC-40, F-actin, MIG-2, and PI(4,5)P<sub>2</sub> polarized normally were invading (Figures 4A, 4C, and 4E; Figure S8). In contrast, *ina-1(gm39)* mutant ACs that had significant reductions in the polarized distribution and membrane localization of UNC-40 and other invasive membrane components did not invade (Figures 4B, 4D, and 4E; Figure S8). The polarity of the invasive membrane components was normal in *ina-1(gm144)* mutants (Figure S5; data not shown),

consistent with this allele not affecting an *ina-1* function necessary for invasion. These results strongly support the notion that the key role of INA-1/PAT-3 in regulating AC invasion is promoting the formation of the invasive membrane. In addition, the positive correlation between the proper localization of UNC-40::GFP and invasion in *ina-1(gm39)* mutants suggests that the integrin and netrin pathways function together to form the invasive membrane.

#### INA-1/PAT-3 and UNC-6 (Netrin) Have Distinct, Synergistic Roles in Invasive Membrane Formation

The effects after reduction or loss of INA-1/PAT-3 function on the invasive membrane differed noticeably from those observed after loss of UNC-6. Whereas the components of the invasive membrane (actin regulators, PI(4,5)P<sub>2</sub>, F-actin, and UNC-40) are not properly polarized in *unc-6* mutants, they still associate with the cell cortex (Ziel et al., 2009). In contrast, loss or reduction of INA-1/PAT-3 appeared to result in an overall decrease in the localization of these molecules to the cell membrane (see Figures 2D–2F and 3F; Figure S6). These observations led us to further compare invasive membrane formation after loss of netrin versus integrin activity.

The assembly of actin filaments is the target of a wide range of signaling networks (Disanza et al., 2005), and a dense cortical F-actin network is a key component of the AC's invasive membrane. Thus, to more definitively assess the relative functions of integrin and netrin signaling on invasive cell membrane formation, we measured the integrated fluorescence intensity of the F-actin probe mCherry::moeABD in wild-type as well as *unc-6(ev400)* and *ina-1(gm39)* mutants that failed to invade at the P6.p four-cell stage. A threshold value was set to measure the volume and amount of the dense F-actin network that composes the invasive membrane of wild-type ACs (see Experimental Procedures). Importantly, the AC-specific promoter *cdh-3* used to drive mCherry::moeABD is not regulated by *ina-1* or *unc-6* and drove similar levels of mCherry::moeABD under all conditions (see Experimental Procedures). Whereas the polarity of the dense F-actin network was perturbed in *unc-6(ev400)* mutants as previously reported (Figures 5A and 5B), the overall estimated volume and amount was similar to that observed in wild-type animals (Figure 5D). In *ina-1(gm39)* mutants, there was some mispolarization of the F-actin network (Figure 5C), consistent with a reduction of netrin function. The most notable defect, however, was the greater than four-fold loss in the total volume and amount of the dense F-actin network (Figures 5C and 5D; Movies S3–S5), suggesting that INA-1/PAT-3 regulates F-actin recruitment or polymerization at the cell membrane. These results indicate that integrin and netrin have distinct roles that act together to properly form the invasive cell membrane: INA-1/PAT-3 plays a broad role in promoting the membrane association of invasive membrane components (including the netrin receptor UNC-40), whereas netrin signaling specifically orients these molecules toward the BM. Further supporting this cell biological evidence of a synergistic function for these pathways in invasive membrane formation, we detected a strong synergistic genetic interaction between *ina-1(gm39)* and *unc-40(e271)* mutants. Whereas 22% and 20% ACs in singly mutant *ina-1(gm39)* and *unc-40(e271)* animals failed to invade at the P6.p eight-cell stage, respectively, ACs in an *ina-1(gm39);*



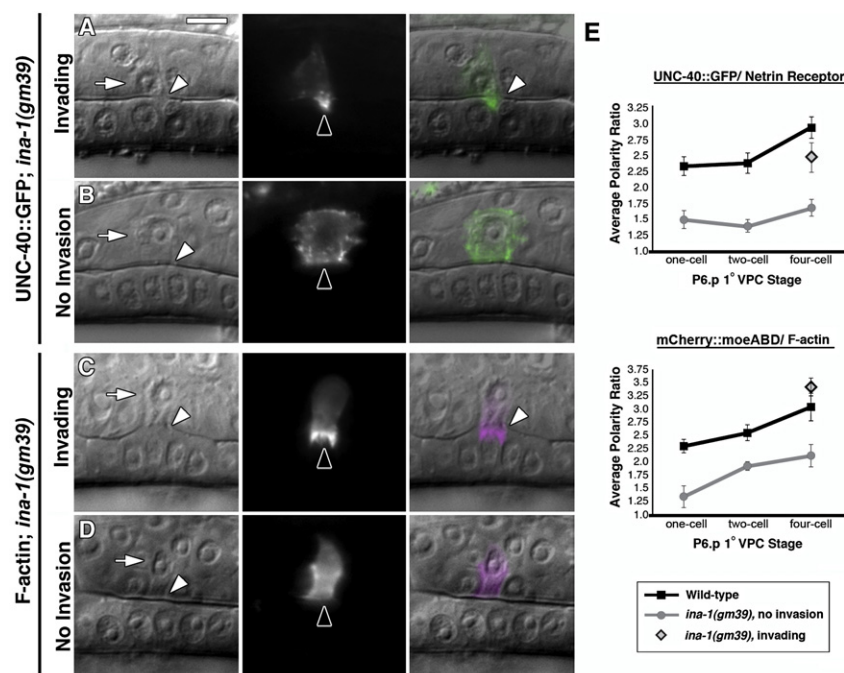


**Figure 4. Invasive Membrane Formation in *ina-1(gm39)* Hypomorphs Correlates with Invasion**

Nomarski image (left); corresponding fluorescence (center); overlay (right).

(A) ACs had UNC-40::GFP polarized at the site of invasion (black arrowhead) in *ina-1(gm39)* mutants that were invading (white arrowheads).

(B) In contrast, UNC-40::GFP polarity was absent or reduced (black arrowhead) in ACs that failed to invade (white arrowhead).

(C) Similarly, the F-actin probe mCherry::moeABD was polarized to the invasive membrane (black arrowhead) in *ina-1(gm39)* mutant ACs in the process of invading (white arrowheads).

(D) F-actin was perturbed (black arrowhead) in ACs that did not invade (white arrowhead).

(E) Quantification of UNC-40::GFP (top) and F-actin (bottom) polarization to the invasive cell membrane in wild-type (black squares), *ina-1(gm39)* mutants that failed to invade (gray circles), and *ina-1(gm39)* mutants that invaded at the P6.p four-cell stage (gray diamonds;  $n \geq 18$  animals for each stage). In *ina-1(gm39)* ACs that failed to invade, the polarity of UNC-40::GFP and F-actin was significantly less than wild-type ( $p < 8 \times 10^{-4}$ ; Student's *t* test); however, polarity was similar to wild-type in invading ACs ( $p > 0.05$ , Student's *t* test). Error bars report the standard error of the mean.

*unc-40(e271)* double mutant strain displayed a more severe phenotype than the additive effects of these mutations alone, with a >80% block in invasion (Table 1).

### INA-1/PAT-3 Regulates the Deposition of the FOS-1A Target Hemicentin

Cell invasion through BMs requires the integration of multiple signaling pathways that regulate distinct aspects of invasion. Thus, we examined the interaction of INA-1/PAT-3 with the FOS-1A pathway, a major regulator of BM removal during AC invasion (Hwang et al., 2007; Rimann and Hajnal, 2007; Sherwood et al., 2005). ACs in *fos-1a* mutants still form an invasive cell membrane and extend processes; however, these protrusions fail to break through the BM (Sherwood et al., 2005; Ziel et al., 2009). Treatment of *fos-1(ar105)* animals with *ina-1(RNAi)* enhanced the invasion defect (Table 1), indicating that *ina-1* has functions distinct from the *fos-1a* pathway. Consistent with this notion, transcriptional reporters for FOS-1A and all of its known targets were expressed normally in *HA-βtail* animals (Figures 6A and 6B; data not shown). Conversely, expression of INA-1/PAT-3::GFP was normal after *fos-1(RNAi)* treatment (20/20 animals). Although these data indicate distinct activities during invasion, we have recently shown that the FOS-1A and netrin pathways converge at the invasive membrane to regulate BM removal (Ziel et al., 2009), suggesting that FOS-1A and INA-1/PAT-3 functions might similarly intersect at this crucial subcellular domain.

A key downstream target(s) of FOS-1A function remains to be identified, as null mutations in known FOS-1A targets produce only mild defects in invasion (Sherwood et al., 2005). For example, loss of the FOS-1A target *zmp-1*, which encodes

a matrix metalloproteinase, does not affect AC invasion, and its loss does not enhance the phenotype of *HA-βtail* animals (Table 1). Null mutations in the FOS-1A target hemicentin (*him-4*), a conserved extracellular matrix protein, however, do cause a moderate invasion defect (Table 1). A functional hemicentin::GFP fusion protein is deposited under the invasive cell membrane of wild-type ACs just prior to invasion, where it promotes BM removal (Figures 6C and 6E). Although hemicentin was expressed normally in the AC in *HA-βtail* animals (Figure 6B), it was not assembled under the AC's invasive membrane in >95% of these animals (93/99 animals; Figures 6D and 6F). RNAi targeting *ina-1*, *pat-3*, or *talin* caused similar reductions in hemicentin deposition, whereas expression of the control construct HA-βΔ did not affect this process (Figure S9). Furthermore, loss of hemicentin did not enhance the invasion defect of *HA-βtail* animals (Table 1). These results indicate a clear dependency of hemicentin deposition and function on integrin activity and demonstrate that the FOS-1A and integrin pathways intersect at the invasive membrane to regulate BM removal.

### DISCUSSION

Cell invasion through BMs plays crucial roles in normal physiological processes and the dissemination of cancer. We show here that the *C. elegans* integrin heterodimer INA-1/PAT-3 is a key regulator of this process during AC invasion, functioning within the AC to generate the specialized invasive cell membrane. A key element of this function is promoting the activity of the netrin pathway within the AC, which ensures the correct polarization of the invasive front toward the BM.

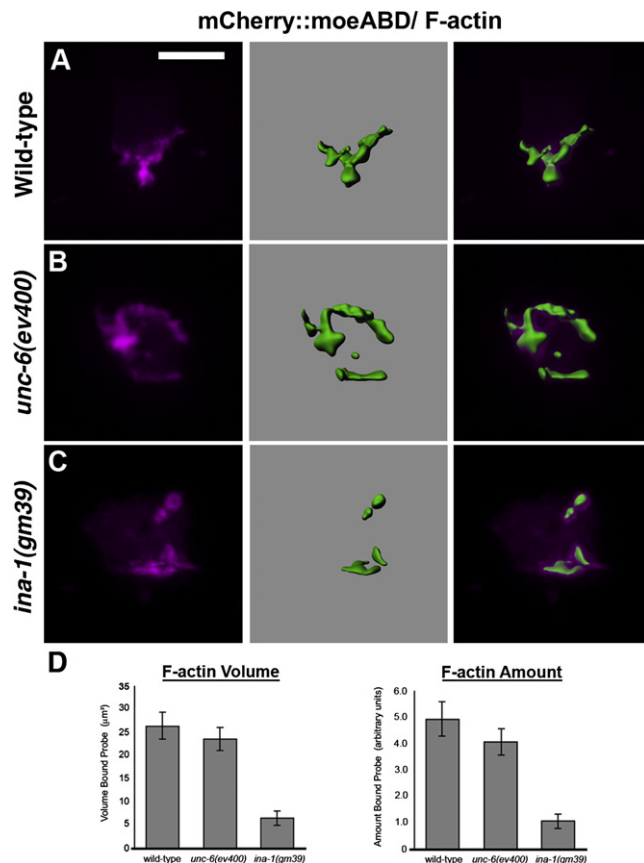


**Figure 5. INA-1/PAT-3 and UNC-6 Differentially Regulate the Dense F-actin Network at the Invasive Membrane**

All animals are viewed at the P6.p four-cell stage. Fluorescence (left), corresponding dense F-actin network shown with isosurface rendering (center), overlay (right).

(A) In wild-type animals, F-actin (mCherry::moeABD) localized to the invasive cell membrane.

(B) In *unc-6* mutants, there was a similar volume and amount of dense F-actin; however, it was mislocalized throughout the cortex of the AC.

(C) *ina-1* mutants that failed to invade showed a decreased amount and volume of dense F-actin, as well as mislocalization (see corresponding Movies S3–S5).

(D) Histograms report the volume (left) and amount of the F-actin probe (right) inside isosurface renderings in wild-type, *unc-6(ev400)*, and *ina-1(gm39)* ACs. The volume and amount of bound F-actin probe within the isosurface in *unc-6(ev400)* mutants was similar to wild-type ( $p > 0.05$ ), but was ~four-fold less in the *ina-1* mutants analyzed ( $p < 4 \times 10^{-6}$ ,  $n = 15$  animals for each background, Student's *t* test). Error bars report the standard error of the mean.

### INA-1/PAT-3 Integrin Signaling Mediates BM Invasion In Vivo

Understanding the requirements and potential roles for vertebrate integrins during cell invasion through BMs in vivo has been clouded by loss-of-function phenotypes that are either lethal (Stephens et al., 1995), extremely complex at the cellular and tissue level (Brockbank et al., 2005), or absent because of apparent genetic redundancy (Bader et al., 1998). Compared with at least 24 known integrin heterodimers in vertebrates, only 2 are predicted in *C. elegans*, simplifying genetic analysis of integrin function (Kramer, 2005). Of the two predicted integrin

heterodimers in *C. elegans*, only the INA-1/PAT-3 heterodimer was found to regulate AC invasion. *ina-1*, *pat-3*, *taln*, and *pat-4*(ILK) RNAi-treated animals and *ina-1(gm39)* hypomorphic mutants were defective in AC invasion. Furthermore, tissue-specific RNAi and tissue-specific expression of a dominant-negative form of *pat-3* (HA- $\beta$ tail) in the AC or vulval cells, as well as mosaic analysis in the *pat-3(rh54)* null mutant, revealed that reduction of INA-1/PAT-3 function within the AC blocks invasion, whereas perturbation of INA-1/PAT-3 function in the vulval cells does not affect invasion. The reduction of INA-1/PAT-3 function slightly reduced the contact area of the AC with the BM, consistent with a function for this integrin heterodimer in modulating adhesion. However, the vast majority of ACs that failed to invade were attached to an intact BM, suggesting that the role of INA-1/PAT-3 extends beyond regulating matrix attachment. Taken together, our results indicate an active, cell-autonomous requirement for the INA-1/PAT-3 integrin heterodimer in mediating BM invasion in vivo and support the idea that integrins might function generally in development and cancer to mediate passage through BMs.

### INA-1/PAT-3 Regulates the Formation of a Specialized Invasive Cell Membrane

The membrane structures that cells utilize to migrate through BMs in vivo are poorly understood (Machesky, 2008). The protrusive activity of the AC relies on the formation of a specialized invasive cell membrane containing the netrin receptor UNC-40 (DCC); a number of actin regulators, including the Rac GTPase MIG-2 and the phospholipid PI(4,5)P<sub>2</sub>, as well as F-actin (Ziel et al., 2009). The levels of HA- $\beta$ tail within the AC mirrored perturbations in the invasive membrane: ~5 hr prior to invasion when expression of HA- $\beta$ tail was low, the polarization of UNC-40, MIG-2, PI(4,5)P<sub>2</sub>, and F-actin to the invasive membrane was normal, but as expression levels of HA- $\beta$ tail increased approaching the time of invasion, there was a corresponding decrease in the localization of these components to the invasive front. Reduction of *ina-1*, *pat-3*, and *taln* by RNAi similarly resulted in decreases in the polarity of these markers. These observations suggest that INA-1/PAT-3 has a direct role in regulating the formation of the invasive cell membrane.

INA-1 is most similar to laminin-binding integrins (Baum and Garriga, 1997), consistent with its mediating a direct interaction between the invading AC and its BM target. Furthermore, studies performed in vertebrate cell culture have shown that the cytoplasmic domain of integrins is capable of anchoring a large complex of proteins that regulate Rac localization to the cell membrane, PI(4,5)P<sub>2</sub> generation at the plasma membrane, and cell cortex-associated recruitment and nucleation of F-actin (Delon and Brown, 2007; Wiesner et al., 2005). These studies support a close relationship between INA-1/PAT-3 function and its regulation of the cell membrane association of the Rac MIG-2, the phospholipid PI(4,5)P<sub>2</sub>, and F-actin. Moreover, the positive correlation between the proper localization of these components and the ability of the AC to invade in *ina-1* hypomorphic mutants offers strong evidence that INA-1/PAT3 controls invasion by promoting invasive membrane formation.

Our results showing a clear dependence of UNC-40 (DCC) membrane localization on INA-1/PAT-3 activity might have important implications to integrin-netrin pathway interactions in



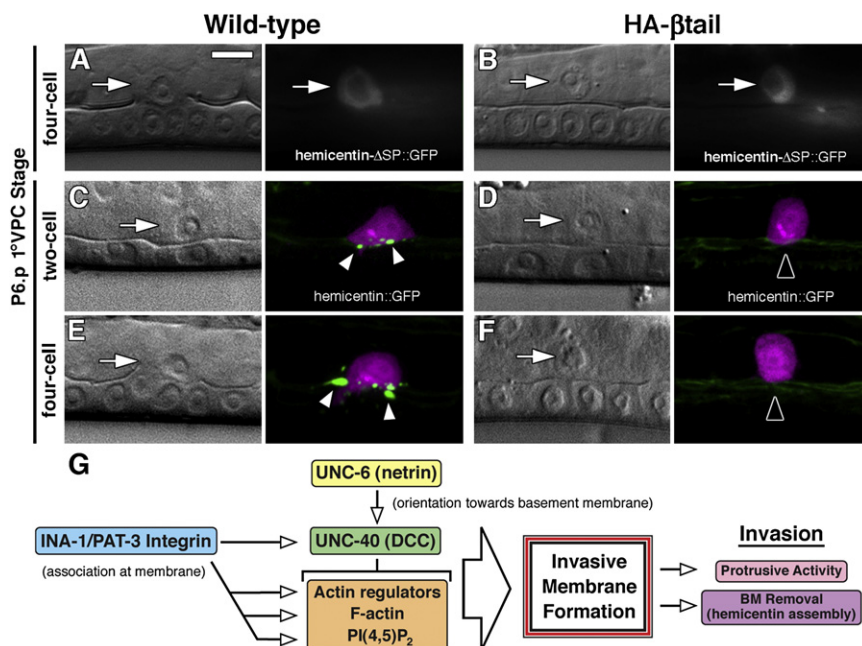


**Figure 6. INA-1/PAT-3 Regulates the Assembly of the FOS-1A Target Hemicentin at the Site of Invasion**

Nomarski image (left); fluorescence (right).

(A) Expression of the transcriptional reporter for the FOS-1A target hemicentin (hemicentin- $\Delta$ SP::GFP) in a wild-type AC.

(B) Similar levels of hemicentin- $\Delta$ SP::GFP were expressed in *HA- $\beta$ tail* ACs.

(C–F) (C and E) In wild-type animals, hemicentin::GFP was deposited in small puncta (white arrowheads) in the BM below the AC during invasion. (D and F) AC-specific expression of *HA- $\beta$ tail* perturbed hemicentin deposition under the AC (black arrowheads).

(G) Schematic diagram of integrin and netrin pathway contributions to invasive membrane formation. INA-1/PAT-3 integrin promotes the membrane association of the netrin receptor UNC-40, actin regulators such as the Rac protein MIG-2 and PI(4,5)P<sub>2</sub>, and F-actin, whereas the netrin pathway orients these components toward the BM. The proper formation of the invasive membrane is required to generate invasive protrusions and assemble hemicentin during invasion.

other contexts. Previous work in vertebrates has indicated that several laminin-binding integrins can act as direct receptors for Netrin-1 (Yebra et al., 2003). It has been postulated that these integrins might act as a coreceptor with DCC in signaling to downstream effectors (Nikolopoulos and Giancotti, 2005), and thus could stabilize DCC localization through this interaction. Although our data do not rule out this possibility, the different patterns of UNC-40 (DCC) localization after loss of UNC-6 versus loss of INA-1/PAT-3 indicate that INA-1/PAT-3 plays a broader role in regulating UNC-40 localization. Specifically, loss of UNC-6 resulted in mispolarization of UNC-40 along all cell membranes, whereas loss of INA-1/PAT-3 led to an overall decrease in membrane localization. These observations support the idea that INA-1/PAT-3 regulates the stabilization or trafficking of UNC-40 at the cell membrane.

We have also found that INA-1/PAT-3 mediates assembly of the extracellular matrix protein hemicentin under the invasive membrane of the AC. Hemicentin is transcribed in the AC and deposited extracellularly at the site of invasion where it promotes breaching of the BM (Sherwood et al., 2005). Expression of *HA- $\beta$ tail* within the AC did not alter hemicentin transcription, but nearly abolished its assembly under the invasive membrane, as did RNAi treatments targeting INA-1/PAT-3 signaling. INA-1/PAT-3 might directly regulate the assembly of hemicentin, similar to known roles for vertebrate integrins in fibronectin matrix deposition (Wierzbicka-Patynowski and Schwarzbauer, 2003). Alternatively, INA-1/PAT-3 could influence hemicentin assembly indirectly through its role in invasive membrane formation. Consistent with the later hypothesis, in *unc-6* mutants, the AC's invasive membrane is mispolarized and hemicentin deposition is decreased and misdirected to other surfaces (Ziel et al., 2009).

In vitro studies have shown that integrins recruit surface proteases toward matrix attachment sites to mediate matrix degradation (Wolf et al., 2003). The only identified protease expressed in the AC during invasion is the matrix metalloproteinase ZMP-1. A

FLAG-tagged ZMP-1 protein is not strongly localized to the invasive membrane, and genetic deletion of *zmp-1* does not perturb AC invasion (Sherwood et al., 2005). Furthermore, we did not detect a genetic interaction between *zmp-1* and *pat-3*. ZMP-1 might function redundantly with other proteases. Alternatively, AC invasion may be predominantly driven by nonproteolytic remodeling of the BM, as has been suggested by experimental observations during the trafficking of leukocytes and the activity of epithelial and carcinoma cell lines in vertebrates (Rabinovitz et al., 2001; Rowe and Weiss, 2008).

### Integrin and Netrin Have Distinct Roles in Invasive Membrane Formation

One of the challenges in understanding the diversity of integrin functions in vivo is elucidating the interactions with other signaling pathways that together mediate specific cellular functions (Wiesner et al., 2005). Our results reveal an interaction between the integrin and netrin pathways within the AC that is required for the proper generation and organization of the invasive cell membrane. Although both UNC-6 and INA-1/PAT-3 participate in the formation of the AC's invasive membrane, their roles in regulating this invasive front are distinct. In *unc-6* mutants, UNC-40 (DCC), actin regulators, PI(4,5)P<sub>2</sub>, and F-actin are still associated with the AC's plasma membrane, but they mispolarize along all surfaces of the AC (Ziel et al., 2009). In contrast, there was a reduction in the membrane targeting of these molecules after perturbation in INA-1/PAT-3 function, but not dramatic mislocalization to other membranes. Taken together, these observations suggest that INA-1/PAT-3 has a function in promoting the membrane association of components of the invasive cell membrane, including the netrin receptor UNC-40, whereas the UNC-6 (netrin) pathway acts to direct or confine these components toward the BM, consistent with a proposed scaffolding function for UNC-40 (DCC) (Gitai et al., 2003; Shekharabi et al., 2005). Strongly supporting cooperative functions for

these pathways in regulating AC invasion, animals harboring mutations in both *unc-40* and *ina-1* showed a synergistic genetic interaction and displayed a more severe block of invasion than the additive defects of these mutants when present alone. A schematic diagram summarizing the role of INA-1/PAT-3 (integrin) and UNC-6 (netrin) pathway function in invasive membrane formation and its role in AC invasion is shown in Figure 6G.

Integrin and netrin pathways play key roles in a number of shared cellular processes involving cell invasion through BMs, including angiogenic vessel sprouting, leukocyte transmigration, and metastatic cancer (Avraamides et al., 2008; Baker et al., 2006; Fitamant et al., 2008; Hodiola-Dilke, 2008; Ly et al., 2005; Nikolopoulos and Giancotti, 2005; Sixt et al., 2006; White and Muller, 2007). These shared functions indicate that the integrin and netrin pathway interaction revealed here might be a common mechanism to generate and polarize an invasive cellular response. The dramatically enhanced block in AC invasion after reduction of function in both pathways further suggests that combined therapeutic targeting of integrin and netrin signaling may provide a powerful strategy by which to modulate cell-invasive behavior in development and human disease.

## EXPERIMENTAL PROCEDURES

Details of tissue-specific expression of dominant-negative *pat-3*, *pat-3*, and *ina-1* expression studies; transgenic animal construction; and P8.p isolation experiments are described in Supplemental Experimental Procedures.

### Worm Handling and Strains

Strains were reared and viewed at 20°C by using standard methods (Brenner, 1974). Wild-type nematodes were strain N2. In the text and figures, we designate linkage to a promoter by using the (>) symbol and linkages that fuse open reading frames by using the (::) annotation. The following transgenes and alleles were used for studies performed in this paper: *qyEx4[zmp-1 > HA-βtail]*, *qyEx9[pat-3::GFP]*, *qyEx35[zmp-1 > HAβΔ]*, *qyEx36[pat-3::GFP; genomic ina-1]*, *qyEx33[pat-3::GFP; genomic ina-1]*, *gmls5[ina-1::GFP]*, *qyEx41[pat-3::GFP; genomic ina-1]*, *qyls42[pat-3::GFP; genomic ina-1]*, *qyls43[pat-3::GFP; genomic pat-2]*, *qyls44[pat-3::GFP; genomic pat-2]*, *qyls25[cdh-3 > mCherry::PLCδ<sup>PH</sup>]*, *syIs157[cdh-3 > YFP]*, *zuls20[par-3::GFP]*, *qyls103[fos-1a > rde-1]*, *qyls110[egl-17 > HA-βtail]*, *qyls125[unc-62 > rde-1]*; **LG1**, *mls27[GFP::mig-2]*, *unc-40(e271)*, *rhIs2[pat-3::GFP]*; **LGII**, *syIs77[zmp-1::YFP]*, *qyls17[zmp-1 > mCherry]*, *qyls23[cdh-3 > mCherry::PLCδ<sup>PH</sup>]*, *rrf-3(pk1426)*; **LGIII**, *dpy-2(e1)*, *pat-3(rh54)*, *ncl-1(e1865)*, *ina-1(gm144)*, *ina-1(gm39)*, *pha-1(e2123ts)*, *unc-119(ed4)*, *rhIs23[hemicentin::GFP]*, *syIs129[hemicentin-ΔSP::GFP]*; **LGIV**, *qyls10[lam-1::GFP]*, *qyls15 [zmp-1 > HA-βtail]*, *qyls48 [zmp-1 > HA-βtail]*, *jcls1[ajm-1::GFP]*; **LGV**, *rde-1(ne219)*, *fos-1(ar105)*, *qyls50[cdh-3 > mCherry::moeABD]*; **LGX**, *syIs123[fos-1a::YFP-TL]*, *him-4(rh319)*, *qyls66[cdh-3 > unc-40::GFP]*, *qyls7[lam-1::gfp]*, *qyls24[cdh-3 > mCherry::PLCδ<sup>PH</sup>]*, *syIs59[egl-17 > CFP]*, *unc-6(ev400)*.

### RNA Interference

A complete analysis of AC invasion defects in genes whose RNAi knockdown produces a Pvl phenotype will be described elsewhere. Double-stranded RNA (dsRNA) targeting *ina-1*, *pat-3*, *talin*, *pat-4*, *pat-2*, and *fos-1* used in this study was delivered by feeding to *rrf-3* and *fos-1(ar105)* mutants as described (Sherwood et al., 2005). RNAi knockdown was confirmed by the presence of an embryonic Pat phenotype and defect in AC invasion; RNAi vectors were sequenced to verify the correct insert. Uterine-specific RNAi was conducted by expressing RDE-1 protein under the control of the *fos-1a* promoter (expressed at the mid-L2 stage through the time of AC invasion) in *rde-1(ne219)* mutants. *rde-1* is a necessary component of the RNAi pathway in *C. elegans*; expression of RDE-1 with tissue-specific promoters in an *rde-1* mutant restores RNAi sensitivity only in the tissue expressing the RDE-1 protein (Qadota et al., 2007).

### Immunolocalization and *zmp-1*-Driven Expression of HA-βtail and HA-βΔ

Transgenic L3-stage animals were synchronized and fixed for HA-βtail and HA-βΔ localization as previously described (Sherwood and Sternberg, 2003). Mouse anti-HA monoclonal antibody clone HA-7 (Sigma) was used at 1:200, and FITC-conjugated goat anti-mouse IgG secondary antibodies (Jackson ImmunoResearch Laboratories) were used at 1:500. Quantification of fluorescence intensity in fixed and stained animals revealed a two-fold higher expression level of HA-βtail in strain *qyls15* versus *qyls48* ( $p < 0.05$ , one-tailed, unpaired t test), consistent with the more severe invasion defect of *qyls15*. Quantification of fluorescence intensity of GFP driven by the AC-specific regulatory element of *zmp-1<sup>mk50-51</sup>* from the P6.p one-cell stage at the early-L3 to the P6.p four-cell stage at mid-L3 showed a 7-fold increase in expression levels of GFP over this time.

### Mosaic Analysis of *pat-3* Function in the AC

To perform a mosaic analysis of *pat-3* function in the AC, 10 ng of the plasmid encoding full-length PAT-3::GFP was injected into *dpy-1(e1) pat-3(rh54) ncl-1(e1865); sDp3(III:f)* animals. Rescued F1 progeny were identified by the Dpy phenotype and PAT-3::GFP. The presence of *pat-3(rh54)* was confirmed in rescued animals by the Pat phenotype. AC invasion was scored at the P6.p four-cell stage, and the presence of the transgene in the AC was determined by the expression of PAT-3::GFP. We were able to detect mosaic loss of the transgene in F1 progeny where maternal contribution of *pat-3* is likely present; however, we were unable to obtain stable F2 lines with mosaic loss of *pat-3* in the vulval cells or AC, possibly reflecting an essential function for stable *pat-3* inheritance for reproduction or viability.

### Microscopy, Image Acquisition, Processing, and Analysis

Images were acquired by using a Yokogawa spinning disk confocal mounted on a Zeiss AxioImager microscope with a 100× Plan-APOCHROMAT objective run by iVision software (Biovision Technologies, Exton, PA) or with a Zeiss AxioImager microscope with a 100× Plan-APOCHROMAT objective equipped with a Zeiss AxioCam MRm CCD camera and run by Axiovision software (Zeiss Microimaging, Inc., Thornwood, NJ). Images were processed and overlaid by using Photoshop 8.0 (Adobe Systems, Inc., San Jose, CA), and three-dimensional projections were constructed by using IMARIS 6.0 (Bitplane, Inc., Saint Paul, MN).

### Scoring of AC Invasion, Polarity, and Fluorescence Intensity

AC invasion was scored as previously described (Sherwood et al., 2005). Polarity in wild-type animals, *ina-1* mutants, RNAi treatments, and HA-βtail animals was determined by using the ratio of the average fluorescence intensity from a five-pixel-wide linescan drawn along the invasive and noninvasive membranes of ACs expressing MIG-2::GFP, UNC-40::GFP, mCherry::moeABD, mCherry::PLCδ<sup>PH</sup>, and PAR-3::GFP strains ( $n \geq 15$  animals for each) by using Image J 1.40 g software. Scoring of apical AJM-1::GFP in the AC was performed as described (Ziel et al., 2009) ( $n = 20$  animals for each). Fluorescence intensities of AC expression of transcriptional reporters for *zmp-1* (*syIs77*), hemicentin (*syIs129*), *cdh-3* (*syIs157*), and translational reporters for *fos-1a* (*syIs123*) and hemicentin (*rhIs23*) were determined by using Image J 1.40 g software ( $n = 15$  animals for each). In all cases, a two-tailed, unpaired Student's t test was used to determine statistical significance of changes in expression or polarity.

### Quantitative F-Actin Measurements

Three-dimensional reconstructions were generated from confocal z-stacks of ACs expressing the F-actin probe mCherry::moeABD by using Imaris 6.0 (Bitplane, Inc., Saint Paul, MN). Isosurface renderings of mCherry::moeABD were created by setting a threshold fluorescence intensity value such that the renderings were constructed only in place of the dense network of F-actin at the invasive membrane of wild-type ACs. Identical settings were used in *unc-6(ev400)* and *ina-1(gm39)* mutants. Quantitative measurements of the volume and integrated fluorescence intensity inside isosurface renderings were made by using the Imaris 6.0 software package ( $n = 15$  animals for each background). Quantification of the total levels of mCherry::moeABD present in the AC in wild-type, *unc-6*, and *ina-1* mutants confirmed similar levels of expression in all three backgrounds.

## SUPPLEMENTAL DATA

Supplemental Data include nine figure, five movies, and Supplemental Experimental Procedures and can be found with this article online at [http://www.cell.com/developmental-cell/supplemental/S1534-5807\(09\)00247-0](http://www.cell.com/developmental-cell/supplemental/S1534-5807(09)00247-0).

## ACKNOWLEDGMENTS

We are grateful to J. Schwarzbauer for the *pat-3* HA- $\beta$ tail vector and PAT-2::GFP strain; J. Plenefisch for the  $\beta$ PAT-3::GFP vector; S. Johnson for imaging advice; the *Caenorhabditis* Genetics Center for providing strains; and N. Sherwood, J. Croce, and D. Matus for comments on the manuscript. This work was supported by a Basil O'Connor Award, Pew Scholars Award, and National Institutes of Health Grant GM079320 to D.R.S.

Received: November 2, 2008

Revised: April 30, 2009

Accepted: June 9, 2009

Published: August 17, 2009

## REFERENCES

- Avraamides, C.J., Garmy-Susini, B., and Varnier, J.A. (2008). Integrins in angiogenesis and lymphangiogenesis. *Nat. Rev. Cancer* 8, 604–617.
- Bader, B.L., Rayburn, H., Crowley, D., and Hynes, R.O. (1998). Extensive vasculogenesis, angiogenesis, and organogenesis precede lethality in mice lacking all  $\alpha$  v integrins. *Cell* 95, 507–519.
- Baker, K.A., Moore, S.W., Jarjour, A.A., and Kennedy, T.E. (2006). When a diffusible axon guidance cue stops diffusing: roles for netrins in adhesion and morphogenesis. *Curr. Opin. Neurobiol.* 16, 529–534.
- Baum, P.D., and Garriga, G. (1997). Neuronal migrations and axon fasciculation are disrupted in *ina-1* integrin mutants. *Neuron* 19, 51–62.
- Brenner, S. (1974). The genetics of *Caenorhabditis elegans*. *Genetics* 77, 71–94.
- Brockbank, E.C., Bridges, J., Marshall, C.J., and Sahai, E. (2005). Integrin  $\beta$ 1 is required for the invasive behaviour but not proliferation of squamous cell carcinoma cells in vivo. *Br. J. Cancer* 92, 102–112.
- Delon, I., and Brown, N.H. (2007). Integrins and the actin cytoskeleton. *Curr. Opin. Cell Biol.* 19, 43–50.
- Disanza, A., Steffen, A., Hertzog, M., Frittoli, E., Rottner, K., and Scita, G. (2005). Actin polymerization machinery: the finish line of signaling networks, the starting point of cellular movement. *Cell. Mol. Life Sci.* 62, 955–970.
- Even-Ram, S., and Yamada, K.M. (2005). Cell migration in 3D matrix. *Curr. Opin. Cell Biol.* 17, 524–532.
- Felding-Habermann, B. (2003). Integrin adhesion receptors in tumor metastasis. *Clin. Exp. Metastasis* 20, 203–213.
- Fitamant, J., Guenebeaud, C., Coissieux, M.M., Guix, C., Treilleux, I., Scoazec, J.Y., Bachelot, T., Bernet, A., and Mehlen, P. (2008). Netrin-1 expression confers a selective advantage for tumor cell survival in metastatic breast cancer. *Proc. Natl. Acad. Sci. USA* 105, 4850–4855.
- Friedl, P., and Wolf, K. (2003). Tumour-cell invasion and migration: diversity and escape mechanisms. *Nat. Rev. Cancer* 3, 362–374.
- Gitai, Z., Yu, T.W., Lundquist, E.A., Tessier-Lavigne, M., and Bargmann, C.I. (2003). The netrin receptor UNC-40/DCC stimulates axon attraction and outgrowth through enabled and, in parallel, Rac and UNC-115/AbLIM. *Neuron* 37, 53–65.
- Hodivala-Dilke, K. (2008).  $\alpha$ v $\beta$ 3 integrin and angiogenesis: a moody integrin in a changing environment. *Curr. Opin. Cell Biol.* 20, 514–519.
- Hood, J.D., and Cheresch, D.A. (2002). Role of integrins in cell invasion and migration. *Nat. Rev. Cancer* 2, 91–100.
- Hotary, K., Li, X.Y., Allen, E., Stevens, S.L., and Weiss, S.J. (2006). A cancer cell metalloprotease triad regulates the basement membrane transmigration program. *Genes Dev.* 20, 2673–2686.
- Hughes, S.M., and Blau, H.M. (1990). Migration of myoblasts across basal lamina during skeletal muscle development. *Nature* 345, 350–353.
- Hwang, B.J., Meruelo, A.D., and Sternberg, P.W. (2007). *C. elegans* EVI1 proto-oncogene, EGL-43, is necessary for Notch-mediated cell fate specification and regulates cell invasion. *Development* 134, 669–679.
- Kalluri, R. (2003). Basement membranes: structure, assembly and role in tumour angiogenesis. *Nat. Rev. Cancer* 3, 422–433.
- Kamath, R.S., Fraser, A.G., Dong, Y., Poulin, G., Durbin, R., Gotta, M., Kanapin, A., Le Bot, N., Moreno, S., Sohrmann, M., et al. (2003). Systematic functional analysis of the *Caenorhabditis elegans* genome using RNAi. *Nature* 421, 231–237.
- Kao, G., Huang, C.C., Hedgecock, E.M., Hall, D.H., and Wadsworth, W.G. (2006). The role of the laminin  $\beta$  subunit in laminin heterotrimer assembly and basement membrane function and development in *C. elegans*. *Dev. Biol.* 290, 211–219.
- Kimble, J. (1981). Alterations in cell lineage following laser ablation of cells in the somatic gonad of *Caenorhabditis elegans*. *Dev. Biol.* 87, 286–300.
- Kramer, J.M. (2005). Basement membranes. In *WormBook, The C. elegans Research Community*, ed. doi/10.1895/wormbook.1.16.1, <http://www.wormbook.org>.
- LaFlamme, S.E., Thomas, L.A., Yamada, S.S., and Yamada, K.M. (1994). Single subunit chimeric integrins as mimics and inhibitors of endogenous integrin functions in receptor localization, cell spreading and migration, and matrix assembly. *J. Cell Biol.* 126, 1287–1298.
- Lee, M., Cram, E.J., Shen, B., and Schwarzbauer, J.E. (2001). Roles for  $\beta$ (pat-3) integrins in development and function of *Caenorhabditis elegans* muscles and gonads. *J. Biol. Chem.* 276, 36404–36410.
- Leptin, M., Bogaert, T., Lehmann, R., and Wilcox, M. (1989). The function of PS integrins during *Drosophila* embryogenesis. *Cell* 56, 401–408.
- Lukashev, M.E., Sheppard, D., and Pytela, R. (1994). Disruption of integrin function and induction of tyrosine phosphorylation by the autonomously expressed  $\beta$  1 integrin cytoplasmic domain. *J. Biol. Chem.* 269, 18311–18314.
- Ly, N.P., Komatsuzaki, K., Fraser, I.P., Tseng, A.A., Prodhon, P., Moore, K.J., and Kinane, T.B. (2005). Netrin-1 inhibits leukocyte migration in vitro and in vivo. *Proc. Natl. Acad. Sci. USA* 102, 14729–14734.
- Machesky, L.M. (2008). Lamellipodia and filopodia in metastasis and invasion. *FEBS Lett.* 582, 2102–2111.
- Marlin, S.D., Morton, C.C., Anderson, D.C., and Springer, T.A. (1986). LFA-1 immunodeficiency disease. Definition of the genetic defect and chromosomal mapping of  $\alpha$  and  $\beta$  subunits of the lymphocyte function-associated antigen 1 (LFA-1) by complementation in hybrid cells. *J. Exp. Med.* 164, 855–867.
- Martin-Bermudo, M.D., and Brown, N.H. (1999). Uncoupling integrin adhesion and signaling: the  $\beta$ PS cytoplasmic domain is sufficient to regulate gene expression in the *Drosophila* embryo. *Genes Dev.* 13, 729–739.
- Nikolopoulos, S.N., and Giancotti, F.G. (2005). Netrin-integrin signaling in epithelial morphogenesis, axon guidance and vascular patterning. *Cell Cycle* 4, e131–e135.
- Qadota, H., Inoue, M., Hikita, T., Koopen, M., Hardin, J.D., Amano, M., Moerman, D.G., and Kaibuchi, K. (2007). Establishment of a tissue-specific RNAi system in *C. elegans*. *Gene* 400, 166–173.
- Rabinovitz, I., Gipson, I.K., and Mercurio, A.M. (2001). Traction forces mediated by  $\alpha$ 6 $\beta$ 4 integrin: implications for basement membrane organization and tumor invasion. *Mol. Biol. Cell* 12, 4030–4043.
- Rescher, U., Ruhe, D., Ludwig, C., Zobiack, N., and Gerke, V. (2004). Annexin 2 is a phosphatidylinositol (4,5)-bisphosphate binding protein recruited to actin assembly sites at cellular membranes. *J. Cell Sci.* 117, 3473–3480.
- Rimann, I., and Hajnal, A. (2007). Regulation of anchor cell invasion and uterine cell fates by the *egl-43* *Evi-1* proto-oncogene in *Caenorhabditis elegans*. *Dev. Biol.* 308, 187–195.
- Risau, W. (1997). Mechanisms of angiogenesis. *Nature* 386, 671–674.
- Rowe, R.G., and Weiss, S.J. (2008). Breaching the basement membrane: who, when and how? *Trends Cell Biol.* 18, 560–574.



- Seydoux, G., Savage, C., and Greenwald, I. (1993). Isolation and characterization of mutations causing abnormal eversion of the vulva in *Caenorhabditis elegans*. *Dev. Biol.* 157, 423–436.
- Sharma-Kishore, R., White, J.G., Southgate, E., and Podbilewicz, B. (1999). Formation of the vulva in *Caenorhabditis elegans*: a paradigm for organogenesis. *Development* 126, 691–699.
- Shekarabi, M., Moore, S.W., Tritsch, N.X., Morris, S.J., Bouchard, J.F., and Kennedy, T.E. (2005). Deleted in colorectal cancer binding netrin-1 mediates cell substrate adhesion and recruits Cdc42, Rac1, Pak1, and N-WASP into an intracellular signaling complex that promotes growth cone expansion. *J. Neurosci.* 25, 3132–3141.
- Sherwood, D.R., and Sternberg, P.W. (2003). Anchor cell invasion into the vulval epithelium in *C. elegans*. *Dev. Cell* 5, 21–31.
- Sherwood, D.R., Butler, J.A., Kramer, J.M., and Sternberg, P.W. (2005). FOS-1 promotes basement-membrane removal during anchor-cell invasion in *C. elegans*. *Cell* 121, 951–962.
- Sixt, M., Bauer, M., Lammermann, T., and Fassler, R. (2006).  $\beta 1$  integrins: zip codes and signaling relay for blood cells. *Curr. Opin. Cell Biol.* 18, 482–490.
- Staun-Ram, E., and Shalev, E. (2005). Human trophoblast function during the implantation process. *Reprod. Biol. Endocrinol.* 3, 56.
- Stephens, L.E., Sutherland, A.E., Klimanskaya, I.V., Andrieux, A., Meneses, J., Pedersen, R.A., and Damsky, C.H. (1995). Deletion of  $\beta 1$  integrins in mice results in inner cell mass failure and peri-implantation lethality. *Genes Dev.* 9, 1883–1895.
- Wang, S., Voisin, M.B., Larbi, K.Y., Dangerfield, J., Scheiermann, C., Tran, M., Maxwell, P.H., Sorokin, L., and Nourshargh, S. (2006). Venular basement membranes contain specific matrix protein low expression regions that act as exit points for emigrating neutrophils. *J. Exp. Med.* 203, 1519–1532.
- White, D.E., and Muller, W.J. (2007). Multifaceted roles of integrins in breast cancer metastasis. *J. Mammary Gland Biol. Neoplasia* 12, 135–142.
- Wierzbicka-Patynowski, I., and Schwarzbauer, J.E. (2003). The ins and outs of fibronectin matrix assembly. *J. Cell Sci.* 116, 3269–3276.
- Wiesner, S., Legate, K.R., and Fassler, R. (2005). Integrin-actin interactions. *Cell. Mol. Life Sci.* 62, 1081–1099.
- Wolf, K., Mazo, I., Leung, H., Engelke, K., von Andrian, U.H., Deryugina, E.I., Strongin, A.Y., Bocker, E.B., and Friedl, P. (2003). Compensation mechanism in tumor cell migration: mesenchymal-amoeboid transition after blocking of pericellular proteolysis. *J. Cell Biol.* 160, 267–277.
- Yebra, M., Montgomery, A.M., Diaferia, G.R., Kaido, T., Silletti, S., Perez, B., Just, M.L., Hildbrand, S., Hurford, R., Florkiewicz, E., et al. (2003). Recognition of the neural chemoattractant Netrin-1 by integrins  $\alpha 6\beta 4$  and  $\alpha 3\beta 1$  regulates epithelial cell adhesion and migration. *Dev. Cell* 5, 695–707.
- Yurchenco, P.D., Amenta, P.S., and Patton, B.L. (2004). Basement membrane assembly, stability and activities observed through a developmental lens. *Matrix Biol.* 22, 521–538.
- Ziel, J.W., Hagedorn, E.J., Audhya, A., and Sherwood, D.R. (2009). UNC-6 (netrin) orients the invasive membrane of the anchor cell in *C. elegans*. *Nat. Cell Biol.* 11, 183–189.